The Effect of Radar Pulse Length on Cloud Reflectivity Statistics

TANEIL UTTAL AND ROBERT A. KROPFLI

NOAA/Environmental Technology Laboratory, Boulder, Colorado

(Manuscript received 27 January 2000, in final form 4 September 2000)

ABSTRACT

When observing clouds with radars, there are a number of design parameters, such as transmitted power, antenna size, and wavelength, that can affect the detection threshold. In making calculations of radar thresholds, also known as minimum sensitivities, it is usually assumed that the radar pulse volume is completely filled with targets. In this paper, the issue of partial beam filling, which results, for instance, if a cloud is thin with respect to the pulse length, or measurements are being made near cloud edges, is investigated. This study pursues this question by using measurements of radar reflectivities made with a 35-GHz, surface-based radar with 37.5-m pulse lengths, and computing how reflectivity statistics would be affected if the same clouds and/or precipitation had been observed with a radar with a 450-m pulse length. In a dataset measured during winter over a mid-continental site, partial beamfilling degraded the percentage of clouds detected by about 22% if it was assumed that the minimum detection threshold was −30 dBZ. In a second dataset collected during summer over a summertime subtropical site that was dominated by thin, boundary layer stratus, partial beam filling degraded the percentage of clouds detected by 38%, again assuming a minimum detection threshold of −30 dBZ. This study provides a preliminary indication of how radar reflectivity statistics from a spaceborne cloud radar may be impacted by design constraints, which would mandate a pulse length of around 500 m and a minimum detection threshold of around −30 dBZ.

1. Background

Clouds have been identified as important modifiers of the earth's radiation balance, and computer models have suggested that the vertical distributions of clouds and cloud properties in the atmosphere are a particularly important factor (Charlock et al. 1992, 1994; Liang and Wang 1997; Slingo and Slingo 1988; Stephens and Webster 1994). These studies indicate that the kind of vertically integrated cloud measurements that are presently being made from satellites with passive remote sensors are not sufficient to observationally quantify the effects of clouds on atmospheric radiation budgets. As pointed out by Schneider and Stephens (1996), the present capability to model vertical distributions of atmospheric cloudiness far exceeds the present capability to observe vertical distributions of atmospheric cloudiness. In response to this quandary, a radar has been designed that could be deployed on a satellite in order to gather the requisite three-dimensional cloud information from space (Walter et al. 1998).

The design of a space-based radar system will need to balance the restrictions of limited antenna size and power, which will be mandated by the satellite platform, against the percentage of clouds that the system will fail to adequately characterize. On the one hand, the kind of short wavelength radars (94 or 35 GHz) that will be supportable on meteorological satellites in the near future will have some attenuation problems and will be unable to penetrate thick high reflectivity clouds and areas of precipitation, resulting in degraded reflectivity measurements and inaccurate echo boundaries. On the other hand, comparisons between coincident radar and lidar data indicate that there will also be clouds that are geometrically thin and/or with small enough particles that will have backscatter characteristics lower then the minimum detection threshold of any radar; these clouds would be missed altogether by such radars. Given the importance of having a space radar to resolve issues of vertical distributions of global cloudiness, the engineering challenge will be to detect a reasonable percentage of the clouds that are expected to be important to radiation studies.

Lemke et al. (1997) and Schneider and Stephens (1996) have used models to estimate the minimum optical depths and cloud covers needed to result in radiatively important clouds, which were defined as clouds sufficient to produce at least a 10 W m^{-2} change at the top of the atmosphere or at the surface, and a handful of observational studies have made estimates of the minimum reflectivity thresholds and pulse lengths[1] that will

Corresponding author address: Taneil Uttal, R/E/ET6, NOAA/Environmental Technology Laboratory, 325 Broadway, Boulder, CO, 80305-3328.
E-mail: Taneil.Uttal@noaa.gov

[1] The *pulse length* determines the fundamental sampling resolution

be necessary for a spaceborne radar to meet the goal of detecting radiatively important clouds. For example, both Atlas et al. (1995) and Brown et al. (1995) used aircraft observations made in ice clouds to calculate radar reflectivities for clouds observed in Kwajalein, Wisconsin, northern Scotland, and over the ocean near Fiji. Model calculations were used to determine which of the observed clouds were radiatively important and, on that basis, the percentage of radiatively important clouds that would be detected by a hypothetical spaceborne radar if −30 and −40 dB*Z* minimum thresholds were utilized was calculated. Brown et al. (1995) concluded that for all-ice clouds, a −30 dB*Z* threshold would be sufficient to detect about 92%–99% of all radiatively important clouds; however, the Atlas et al. (1995) study concluded that a −30 dB*Z* threshold would detect only between 64% and 84% of radiatively important clouds. It is not clear if these significantly different conclusions result from the limited size of the different aircraft datasets and real differences between the observed clouds, or in differences in the model criteria for defining radiatively important clouds. Fox and Illingworth (1997) extended the study to liquid water clouds using radar reflectivities calculated from aircraft measurements made in clouds over the coastal British Isles and around the Azores Archipelago. They concluded that a −30 dB*Z* threshold would detect most radiatively important clouds.

Each of these three studies was based entirely upon radar reflectivities inferred from limited cloud microphysical measurements made from cloud probes mounted on aircraft. In contrast, Lemke et al. (1997) used a general circulation model (ECHAM4) to generate a three-dimensional global cloud dataset that included information on cloud liquid and ice water contents. Using empirical relationships relating reflectivity in units of dB*Z* to cloud liquid and ice contents, a globally distributed field of three-dimensional radar reflectivities was generated and again evaluated against criteria for radiatively important clouds as defined by a model. On average Lemke et al. (1997) found that a −30 dB*Z* threshold detected between 40% and 81% of radiatively important clouds, and a −40 dB*Z* threshold was shown to detect between −77% and 94% of radiatively important clouds. It should be clearly noted that none of the above studies utilized direct measurements of reflectivities in clouds made with a radar, but relied on proxy in situ observational and theoretical datasets.

There has also been some discussion of the required vertical spacing of space-based radar measurements. For instance, modeling work by Stackhouse and Stephens (1991) has indicated that 500 m is a sufficient vertical resolution for cloud boundary detection in terms of calculating the radiative effects of cloud bases and tops. This study, however, addressed only the issue of a 500-m error in specifying the altitude of the cloud. Another important and separate issue is that of partial filling of the radar pulse volume, which results when thin clouds or cloud edges do not completely fill the radar pulse volume, with the magnitude of the partial beamfilling effect being a strong function of the relation between the average cloud thickness and pulse length. Partial beamfilling is illustrated in Fig. 1 where it is shown how underestimates of cloud reflectivity would result as clear air regions are intermixed with cloudy regions within one pulse volume. The potential effects of partial beamfilling were discussed by Brown et al. (1995); however, that study was concerned only with the effects of potential biases in the resulting calculations of ice water contents. They assumed in their calculations that degraded reflectivities were always above the detection threshold of the hypothetical radar.

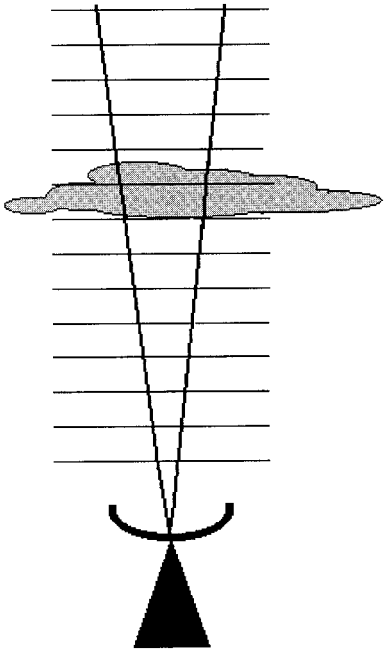

FIG. 1. A schematic illustrating how clouds can partially fill radar pulse volumes.

Mace et al. (1997) generated some statistics on cirrus cloud morphology using two months of vertically pointing, surface-based, 94-GHz radar data gathered over Pennsylvania in the winter of 1994. Although this is not the only recent study to have looked at cloud properties with millimeter-wave radar, it was the first where partial beamfilling effects were examined explicitly using actual radar data. For the 2-month study period, the percentage of time during which cirrus clouds were observed was calculated for both the original dataset, and

with which a radar can collect data and should not be confused with *range gate spacing*, which specifies the range intervals at which the radar video signal is sampled. It is, however, common for range samples to be spaced by an amount equal to the transmitted pulse length giving contiguous sampling at the fundamental resolution of the radar.

TABLE 1. Comparison of operating characteristics of NOAA/ETL 35-GHz radar and proposed space radar.

Feature	NOAA/ETL 35-GHz radar	Proposed space radar
Frequency	34.64 GHz	94 GHz
Doppler	Yes	No
Scanning	Yes	No
Pulse coding	No	Yes
Transmitter	Magnetron	Klystron
Peak transmitted power	80 kW	1.5 kW
Duty cycle	0.1%	1.2%
Antenna diameter	1.2 m	2 m
Beamwidth	0.5°	0.1°
No. of gates	328	120
Estimated sensitivity	−36 dBZ at 5 km AGL	−27 to −30 dBZ
Pulse repetition frequency	Variable—usually 2000 s^{-1}	3500 s^{-1}
Beam diameter at 10 km MSL	87 m	740 m
Pulse length	0.25 μs (37.5 m)	3.33 μs (500 m)

for a reprocessed dataset in which the vertical and horizontal resolutions were degraded to match observations made with a theoretical satellite radar with a 500-m pulse length, a −36 dBZ minimum reflectivity threshold, and a 3-km horizontal footprint. In the original dataset cirrus were observed 32% of the time, and in the resampled dataset, cirrus were observed above the threshold 21% of the time, suggesting that a space-based radar would have seen about two-thirds of the clouds that would have been detected with the shorter pulse length ground-based system. In the Mace et al. (1997) study, the dataset was edited so that only cirrus clouds were included in the statistics.

In this study, we also examine data collected by a surface-based, vertically pointing Doppler radar. As with Mace et al. (1997), the original datasets are computationally resampled to produce the ''virtual'' reflectivity measurements that would result from radar with longer pulse lengths. This dataset is not edited to preclude certain clouds types, and no horizontal averaging based on advective wind speeds to match a horizontal satellite footprint is attempted, because it is the intent of this study to concentrate solely on the effect of vertical resolution. Because 500 m is the operational pulse length that is presently being proposed for a space-based radar (IGPO 1994), we have examined the reflectivity statistics of an effective pulse length of 450 m (a convenient multiple of 37.5 m, which is the operational pulse length of the original dataset) as compared to the reflectivity statistics of the original data gathered with a pulse length of 37.5 m. This study complements the Mace et al. (1997) study by extending the database of observed cloud reflectivities with a surface-based radar to two additional geographical locations; however, it is more inclusive of liquid water clouds and precipitation, and is explicit in demonstrating the altitude dependence of the effects of partial beamfilling.

2. Ground-based radar datasets

a. System description and observations

In the last decade, new millimeter-wave technology has resulted in the development of a number of ground-based radar systems (Clothiaux et al. 1995; Sekelsky and McIntosh 1996; Lhermitte 1987; Kropfli and Kelly 1996) operating at either 35 or 94 GHz (atmospheric window regions). These high-frequency radars have proven to be extremely effective in the observation of nonprecipitating and lightly precipitating clouds throughout the depth of the troposphere (Kropfli et al. 1995; Uttal et al. 1995; Mace et al. 1997, 1998). These radars were initially operated episodically for short-term field experiments. However, unattended, millimeter-wave radars with the capability of collecting long-term datasets over several annual cycles (Moran et al. 1998) have been in operation since November 1996.

In this study, we examine two of the short-term datasets collected by the National Oceanic and Atmospheric Administration (NOAA) Environmental Technology Laboratory (ETL) research grade, 35-GHz radar (NOAA/K), which was operated in Coffeyville, Kansas, during the National Atmospheric and Space Administration (NASA) First ISCCP Regional Experiment II (FIRE II), and then again in Porto Santo, Portugal, during the NASA Atlantic Stratocumulus Transition Experiment (ASTEX). During the FIRE II experiment, the radar was not operated continuously; however, on-site operators collected data whenever clouds were observed visually. The ASTEX experiment was the first deployment with this radar where data were collected around the clock for the entire period of the experiment. Both experiments lasted for about one month. The NOAA/K radar is a scanning Doppler radar, but for both of these experiments it was operated primarily with a fixed elevation angle of 90° (vertically pointing). The short periods during these two experiments when scans were performed are not included in the current study.

The Kansas experiment generated a wintertime midlatitude, continental cloud dataset, while ASTEX produced data on summertime, subtropical, maritime clouds. Approximately 108 h of operational radar data were obtained during FIRE II with clouds spread over 17 nonconsecutive days. These data captured a substantial fraction of the clouds that occurred overhead, with possible exceptions of subvisible cirrus and some nighttime cloudiness. The

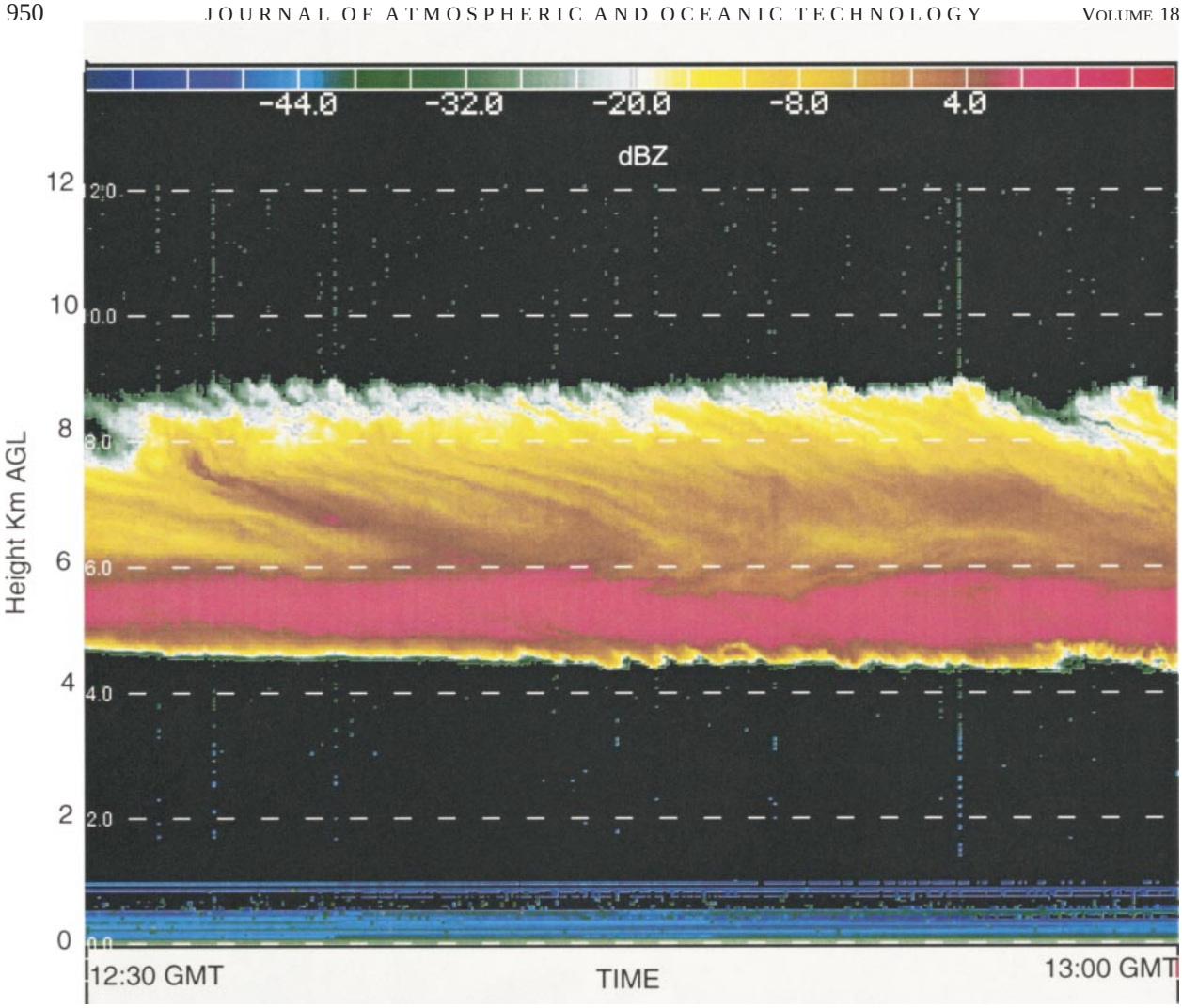

FIG. 2. Thirty-minute time–height cross section of radar reflectivities. Height axis ranges from 0 to 12 km, and time axis ranges from 1230 to 1300 UTC on 21 Nov 1991. Location is Coffeyville, Kansas.

ASTEX data represent 650 h of cloud observations over 27 days and were nearly continuous.

While neither of these datasets are long enough to offer climatologically significant information on radar reflectivity statistics, they both are representative of the cloudiness over the two sites during the experiment periods and are sufficient to suggest the potential effects on radar reflectivity statistics that are caused by different radar pulse lengths. The operating characteristics of NOAA/K are compared with characteristics of the proposed space-based radar in Table 1, and Fig. 2 shows an example of a 30-min time–height cross section of radar reflectivities from NOAA/K. It is this type of data with 3-s averages, 37.5-m pulse lengths, and 328 range gates spaced between 0 and 12 km above ground level (AGL) that forms the basis for this study.

b. Data processing issues

To determine the true percentage of clouds in the atmosphere that will be detected by various reflectivity thresholds, it would be necessary to have a radar system (or a combination of radar, lidar, and radiometers) that could detect all clouds in the atmosphere at all times. Although this is not possible, several steps were taken with the NOAA/K data in this study to obtain as much information as possible at lower reflectivity thresholds than usual. This section briefly describes the processing techniques that were employed to extract the maximum amount of information from these measurements.

1) COMBINING INFORMATION FROM SEPARATE RECEIVERS

The NOAA/K radar employs both linear and log receivers, the first of which can detect reflectivities about 10 dB*Z* lower than the latter, but has only about 45 dB*Z* of dynamic range as opposed to 80 dB*Z* of dynamic range for the log receiver. Range dependent reflectivity thresholds, dictated by the noise floor and the saturation levels, for the log and linear channels are illustrated in

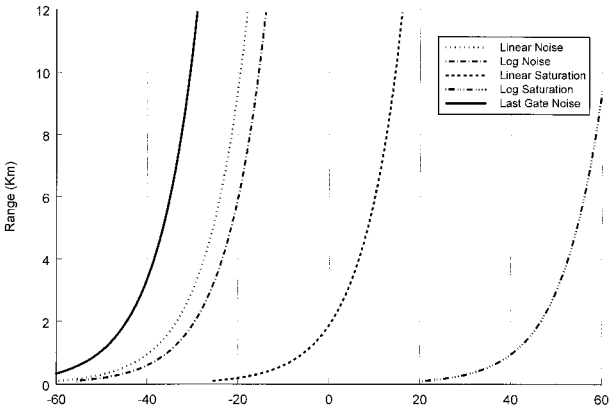

FIG. 3. Range-dependent noise and saturation curves for the log and linear channels on the NOAA/ETL Ka-band radar. The solid curve to the far left shows the approximate minimum detection curve that was utilized in this study by using last gate thresholding techniques.

Fig. 3, which diagrams values obtained from calibrations that are typically performed once or twice for each experiment using a signal from a calibrated source. To take advantage of both channels, measurements from the linear and log channels were combined, after elimination of duplicate values measured by both channels in range dependent, overlap regions.

2) UTILIZATION OF LAST GATE NOISE THRESHOLD

Previous experiments with this radar had focused on accurate absolute reflectivity measurements, and, therefore, the conventional processing utilized noise floors predetermined during a calibration, which discarded measurements with poor signal-to-noise ratios. For this study, it was determined that the minimum acceptable reflectivity could often be significantly lowered by using the measured echo-free signal in the last gate as a threshold, rather than the preset noise value determined from calibration measurements. This ''late-gate'' noise represents the actual system noise, which varies somewhat in time as well as with atmospheric conditions. The solid curve to the left in Fig. 3 shows a measurement of a representative minimum threshold which typifies those used for this study. If a case occurs where there is no detectable radar echo in the last gate, the processing defaults to a preset noise level. This rethresholding allowed the inclusion of measurements for which it was not possible to make good absolute estimates of reflectivity, but for which it was still possible to ascertain that the measurement was in-cloud as opposed to clear air with a high degree of reliability.

3) EFFECTIVE 450-M PULSE LENGTH SAMPLES FROM MEASURED 37.5-M PULSE LENGTH SAMPLES

To create 450-m effective pulse lengths, each original profile of reflectivities was computationally resampled by taking the antilogarithm of the dB*Z* values, averaging the reflectivity values in 12 consecutive gates,[2] and then taking the logarithm to create new reflectivity values for a ''virtual'' 450-m pulse volume. No attempt was made to time average the reflectivity profiles to approximate a horizontal satellite footprint of many kilometers, or the 740-m beamwidth that would be observed from a space radar (Table 1), so the results reported here strictly represent the effect of changing the pulse length from 37.5 to 450 m. In this paper, we examine the statistics of cloud reflectivites below −30 dB*Z*, which is a reflectivity threshold proposed for a spaceborne radar, and −38 dB*Z*, which is a more sensitive limit that could be achieved with pulse-coding techniques, a means to increase sensitivity without degrading the radar resolution by increasing the radar bandwidth.

3. Results

Figure 4 shows the frequency distribution of reflectivities as a function of altitude for the 30-min time–height cross section of radar reflectivities shown in Fig. 2. The shape of this distribution was typical for clouds with bases above 2 km during FIRE II, with reflectivities increasing rapidly in the lowest 200–300 m of the cloud, indicating either a sampling artifact from beamfilling effects even with the 37.5-m pulse length and/or a real microphysical effect from sublimation at cloud base. Reflectivity is then seen to decrease from just above cloud base to cloud top. In this case, the rate of reflectivity decrease with height was approximately 10 dB*Z* km^{-1}, and most likely is primarily a function of the sixth-order dependance of reflectivities on particle size. Assuming that the concentration and phase effects on reflectivity values are minimal, the mean particle diameter would need to decrease by approximately 50% with each kilometer of altitude to produce the observed reflectivity profile.

a. FIRE II

The reflectivity frequency distribution for the entire FIRE II dataset collected with 37.5-m pulse lengths is shown in Fig. 5a. To account for the varying number of in-cloud observations at each height, the reflectivity frequency distributions at each height level are normalized to percentages (with 1 dB*Z* bins). For FIRE II the number of observations at each height was not particularly variable; therefore, the Fig. 5a looks quite similar to the nonnormalized frequency of occurrence histogram (not shown). Some discontinuities in the reflectivity distributions can be seen near the lowest detectable reflectivity values, which increase in value with increasing height. In these areas, absolute measurements of reflectivity are uncertain, but they still reliably rep-

[2] Gate 1 is at 150 m AGL, which is the lowest minimum range for reliable velocity measurements.

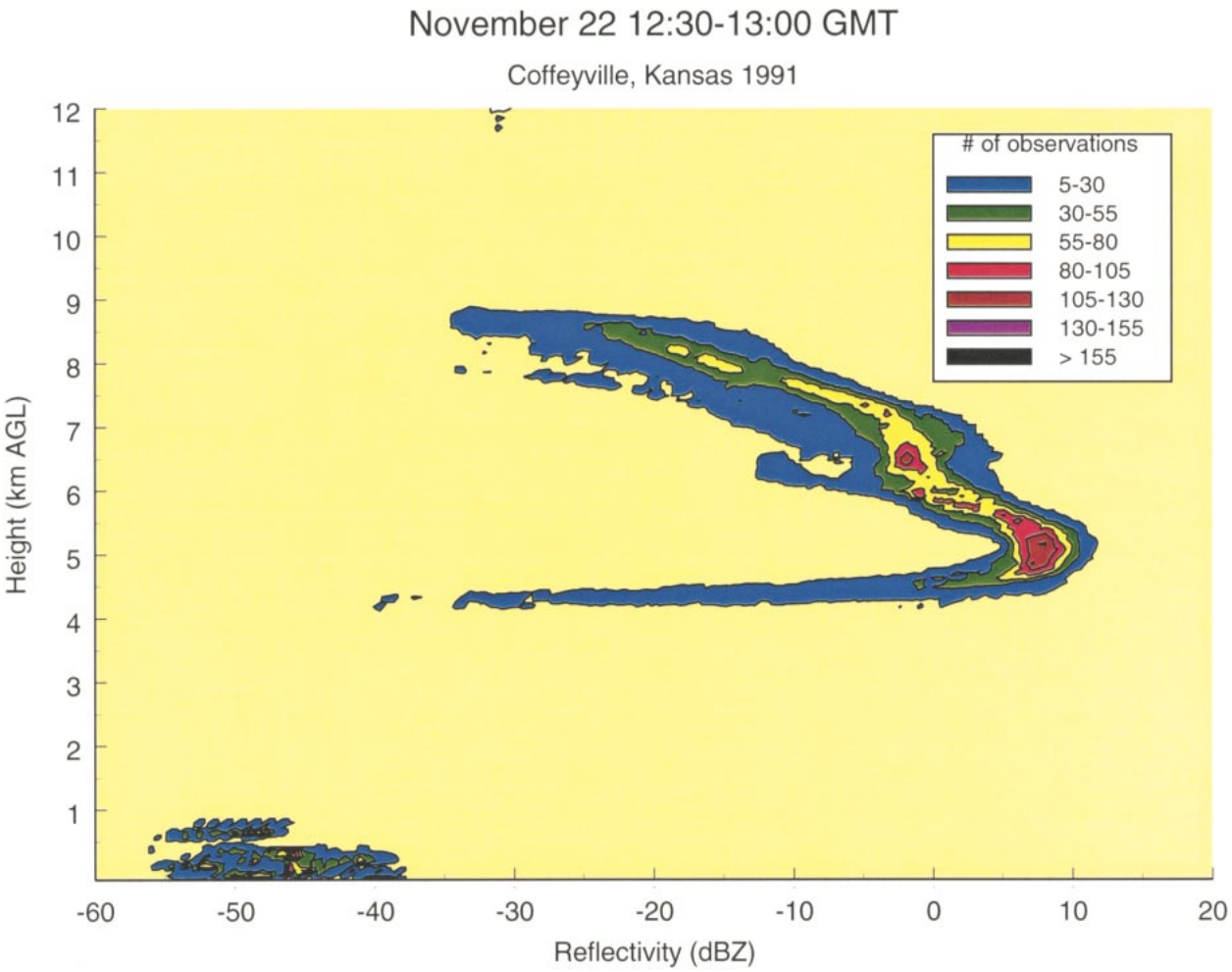

FIG. 4. Frequency of occurrence distribution of observed reflectivity as a function of altitude for the cloud shown in Fig. 2.

resent in-cloud measurements. Below 1 km (all heights AGL), a large number of observations were made of extremely low reflectivity targets (between −45 and −55 dBZ) where cloud measurements are contaminated with very weak ground clutter or signals from boundary layer targets such as insects and other airborne noncloud particulates (Martner and Moran 2001). Radar reflectivities for this winter month in Kansas were observed over a wide range of values with the largest range (about 60 dBZ) between 2 and 4 km. Between 1 and 4 km, there was a tendency for reflectivities to increase with altitude. Above 4 km, this trend reversed, and there was a pronounced decrease with height at a rate of about 7.4 dBZ km^{-1}.

Vertically integrated and normalized reflectivity frequency of occurrence functions are shown for both 37.5- and 450-m pulse lengths in Fig. 5b. The reflectivity distribution between −30 and 10 dBZ for the high-resolution data is more representative of clouds throughout the depth of the atmosphere and the smaller peak at about −42 dBZ is the contribution from the low-altitude clutter. This low reflectivity peak is enhanced in the 450-m resolution data for the following reason. The clutter below 1-km altitude is very weak and generally uniform from the surface to just less than 1-km altitude as shown in Fig. 5a. As such, the 450-m vertical averaging will not significantly change the reflectivity values because of the uniformity of the echo. Thus the clutter contribution to the distribution will not be changed by the averaging. Weak and thin cloud echoes with reflectivities less than −30 dBZ will be reduced by the averaging and will be superimposed onto the clutter echoes centered on about −42 dBZ. The frequency of occurrence of cloud echoes in the ranges greater than −30 dBZ are also shifted to lower reflectivities by the degraded resolution.

Reduction in reflectivities as a function of pulse length averaging is also illustrated in Fig. 6a, which shows the average cloud reflectivity profile calculated for both 37.5- and 450-m pulse lengths. Partial beam-filling decreases the average reflectivity profile by about 2 dBZ at nearly all heights. As mentioned previously, a significant fraction of the signal below 1 km is likely to represent radar echo from ground clutter, which dom-

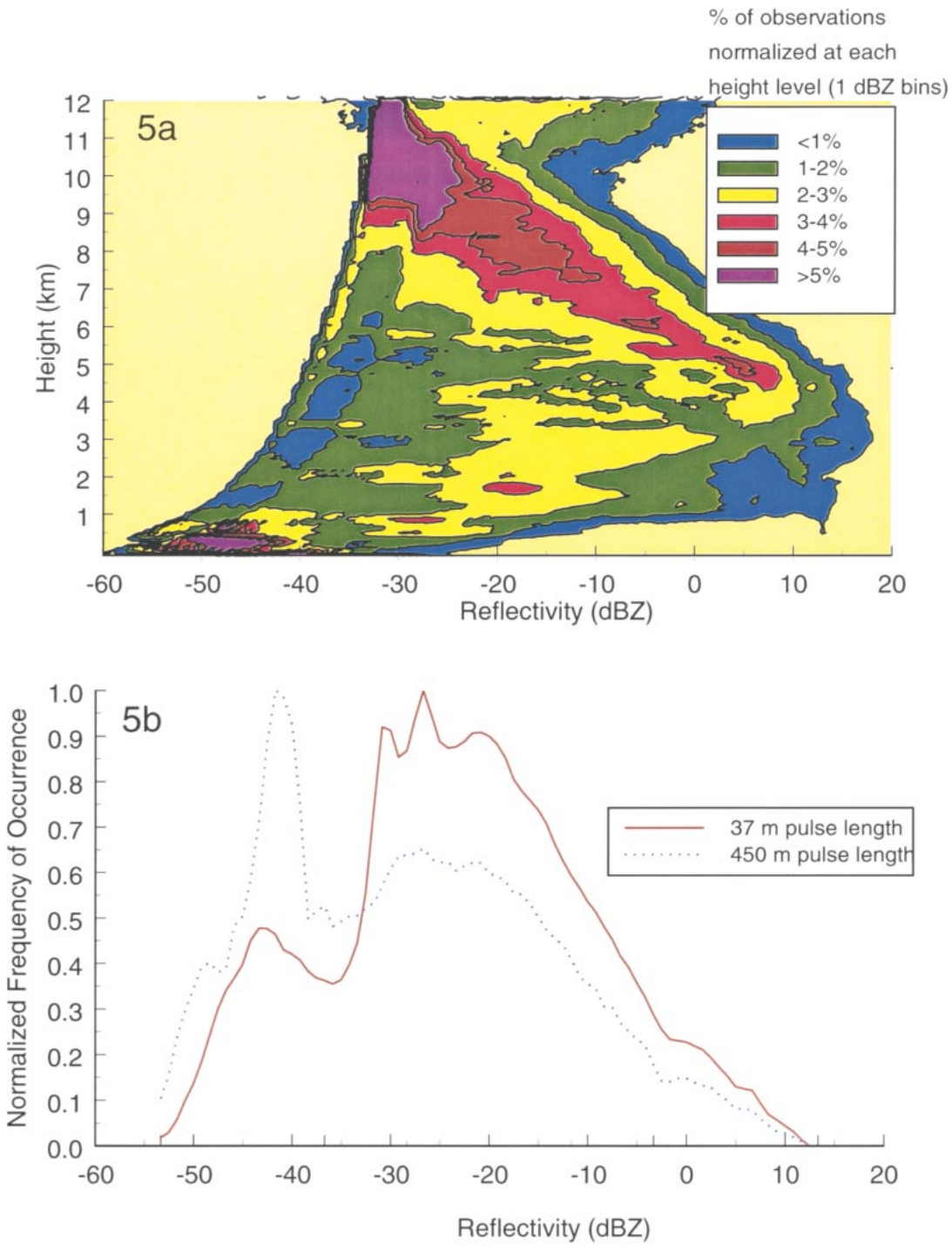

FIG. 5. (a) Frequency of occurrence distribution of reflectivity as a function of altitude for all FIRE II cloud radar observations and (b) total frequency distribution of reflectivities for 37.5-m pulse lengths (solid) integrated over all heights and for 450-m pulse lengths integrated over all heights (dotted).

inates the statistics in that region. The remainder of discussion is confined to altitudes between the heights of 1 and 10 km because of clutter-dominated statistics below 1 km and the small number of samples above 10 km (Fig. 6b).

The total percentage of clouds with reflectivities less than −30 dBZ is shown in Fig. 7a for 37.5- and 450-m pulse lengths at each height level. The 37.5-m pulse length measurements indicate that between about 1.0 km and 4.2 km, the percentage of detectable clouds

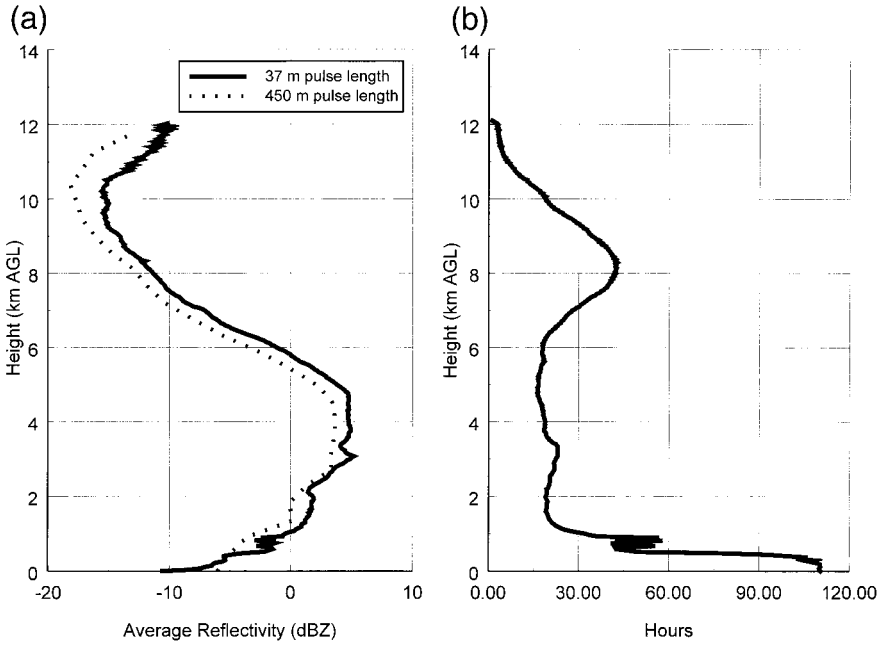

FIG. 6. (a) Profiles of average reflectivity for all FIRE II cloud radar observations for 37.5-m gates (solid) and 450-m gates (dotted) and (b) total hours of observations of clouds as a function of altitude.

below a −30 dBZ threshold ranges from about 45% at 1 km to about 15% at 4 km. Between 4.2 and 8.0 km, about 10% of the detected clouds have reflectivities less than −30 dBZ, and between 8.0 and 10 km, the percentage of clouds with reflectivities less than −30 dBZ increases to 40%. The results do not account for the decreasing sensitivity of the radar with increasing altitude. The values plotted are actually underestimates of the true percentage because of the fraction of undetected clouds that increases with altitude. In spite of this, the

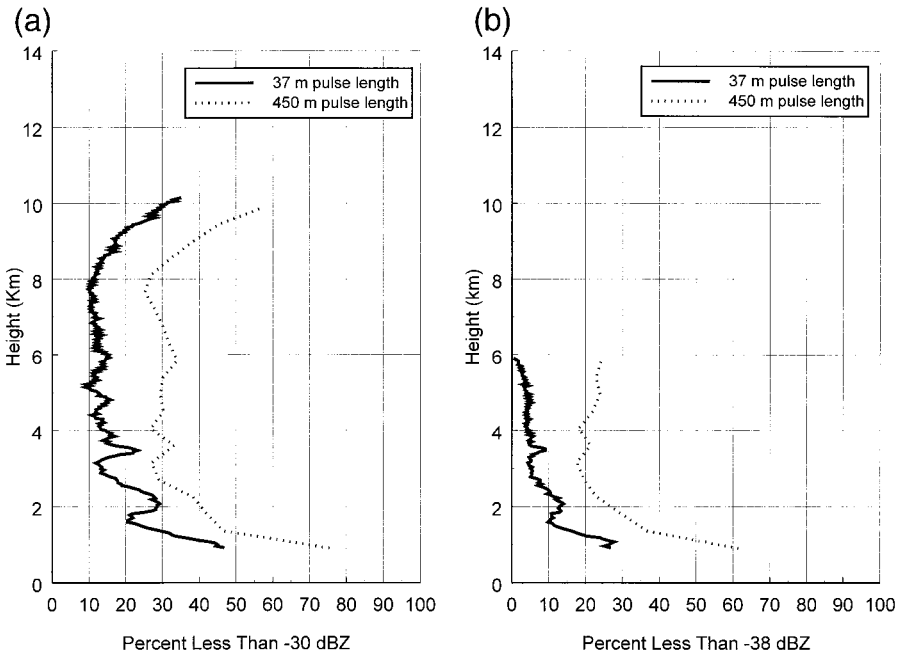

FIG. 7. (a) Percent of observed clouds <−30 dBZ for 37.5-m pulse lengths (solid) and 450-m pulse lengths (dotted) as a function of altitude and (b) percent of clouds less than −38 dBZ for 37.5-m pulse lengths (solid) and 450-m pulse lengths (dotted) as a function of altitude, for FIRE II.

difference between the 37.5-m resolution profiles and the 450-m resolution profiles is expected to be accurate.

For the 450-m pulse length data, the percentage of detectable clouds less than −30 dB*Z* ranges from 78% to 30% between 1 and 4.2 km. Between 4.2 and 8 km, the percentage of clouds less than −30 dB*Z* is about 30%, and above 8 km the percentage increases to 60% at 10 km. The larger fraction of low reflectivity clouds above 8 km is a result of higher cirrus clouds being both thinner and, thus, more susceptible to partial beamfilling problems as well as having lower reflectivities resulting from smaller particles at the colder temperatures. The most important point to draw from Fig. 7a is that the fraction of clouds with reflectivities less than −30 dB*Z* increases by about 20% at all heights because of the degraded range resolution.

The statistics of detectable clouds with reflectivities less than −38 dB*Z* are presented in Fig. 7b. The observations collected with 37.5-m pulse lengths show a decrease in the fraction of clouds with reflectivities less than −38 dB*Z* from 28% at 1 km to 0% at 6 km; no statistics can be calculated above 6 km AGL since that is the altitude at which −38 dB*Z* is the lowest detectable reflectivity limit possible with the NOAA/K radar. Between 2 and 6 km, 10% or less of the clouds have reflectivities less than −38 dB*Z*. For simulated 450-m pulse lengths, the percentage of clouds with reflectivities less than −38 dB*Z* decreases from 60% at 1 km to 30% at 2 km, and ranges between 18% and 26% between 2 and 6 km. Lowering the minimum detection threshold from −30 dB*Z* to −38 dB*Z* appears to increase the percentage of clouds detected by about 15%–20% for the 450-m pulse length dataset. Again, while the percentages of all clouds with reflectivities less than −38 dB*Z* have some error because of some height-dependent fraction of undetectable clouds, the *differences* between the two curves are believed to be representative.

b. ASTEX

The frequency distribution of reflectivities for the ASTEX dataset is presented in Fig. 8a. As for the FIRE II dataset, the observations have been normalized to account for the varying number of in-cloud observations at each altitude, that is, values were normalized to percentages with 1 dB*Z* bins. During the FIRE II experiment this adjustment makes only a small difference to the appearance of the distribution when compared to the distribution of actual occurrences; however, it was more important for the ASTEX dataset. This difference results because of the fact that during FIRE II, clouds were distributed much more evenly throughout the troposphere, whereas during ASTEX the radar echo was nearly always present below 2 km because of the prevalence of marine stratus, and it was significantly more intermittent between 4 and 11 km (Fig. 9b) where altostratus and cirrus were less frequent. Interestingly, the atmosphere between 2 and 4 km over Porto Santo Island was essentially cloud free during June 1992. In contrast to the FIRE II experiment, the measurements of clouds and precipitation below 1 km were not as contaminated by clutter or boundary layer targets. However, ground clutter, which is site dependent, was observed below 300 m during ASTEX. The total integrated reflectivity probability density function for both 37.5- and 450-m pulse lengths is shown in Fig. 8b. As with the FIRE II data, each curve represents all reflectivity values integrated through the depth of the atmosphere and normalized.

The average reflectivity profiles for the 37.5- and 450-m resolution data taken during ASTEX is shown in Fig. 9a. The surface layer stratus clouds below 2 km had average reflectivities of between −20 and −5 dB*Z*, not significantly different from the upper level clouds. The effects of partial beamfilling degrades the average reflectivity profile by about 4 dB*Z*. This difference is larger than for FIRE II (2 dB*Z*) and results from the fact that clouds were, on average, thinner during ASTEX. At 1.9 km, the average reflectivity is reduced by 8–9 dB*Z*; this is the height at which the marine stratus often topped out, and a common altitude for clear air return to be mixed with clouds in the same 450-m pulse length sampling volume. The sharp reflectivity gradient consistently observed here, when included in the 450-m average, significantly reduced the low-resolution reflectivities at this level. The number of hours with observations of marine stratus clouds relative to upper-level cirrus and altostratus clouds is shown in Fig. 9b. Based on the number of available observations and location of clutter, further statistics are calculated only between 300 m–1.9 km and 4–10 km for the ASTEX dataset.

The percentage of NOAA/K detectable clouds with reflectivities less than −30 dBZ for 37.5- and 450-m pulse lengths is shown in Fig. 10a. The 37.5-m measurements show that for the lower-level stratus (<2 km), the percentage of clouds with reflectivities lower than −30 dB*Z* ranged from 40% to 85% between 0.3 and 1.8 km. Again, these percentages are for observed clouds at each level, and do not account for clouds below the detection threshold of the NOAA/K radar. For upper-level clouds, the percentage of clouds less than −30 dB*Z* was 70% at 4 km and 20%–30% between 5 and 10 km. For 450-m pulse lengths, the percentage of clouds with reflectivities less than −30 dB*Z* increases dramatically to between 60% and 95% for clouds below 1.8 km, and 60%–90% between 4 and 10 km. The percentage of clouds detected with the 450-m pulse length dataset is degraded by as much as 35% from the original 37.5-m pulse length dataset.

The percentage of NOAA/K detectable clouds with reflectivities less than −38 dB*Z* are shown for ASTEX

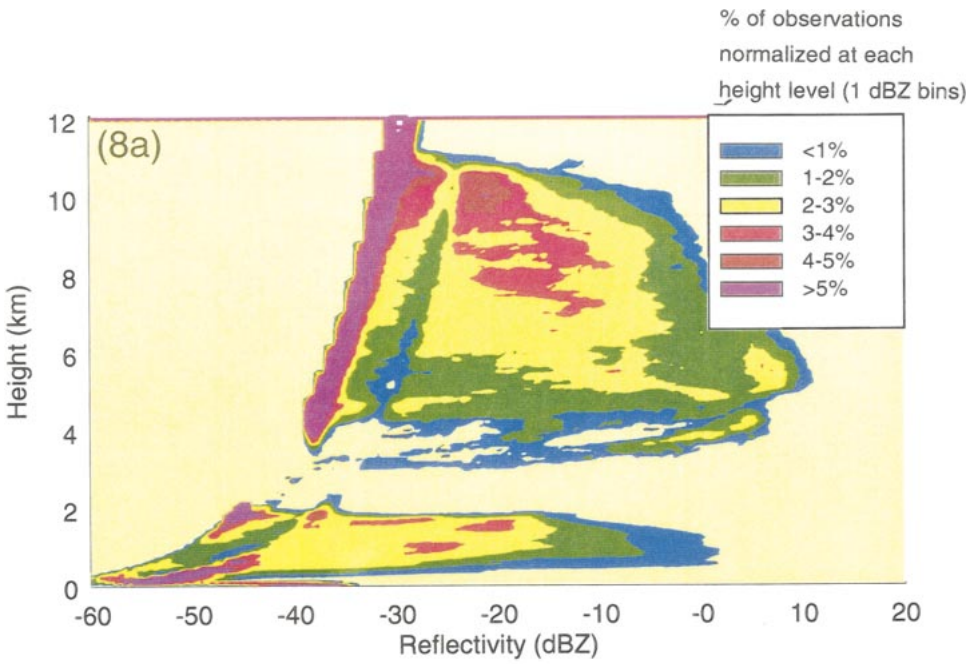

FIG. 8. As in Fig. 5 for ASTEX.

in Fig. 10b. For the low-level clouds, lowering the reflectivity threshold increases the percentage of detected clouds by about 20% for both the 37.5-m pulse lengths observations and for the 450-m pulse length calculations. Statistics are not calculated above 5 km because at that level the minimum detection threshold of the NOAA ETL radar is −38 dBZ.

c. Effects of partial beam filling on individual cloud cases

In addition to monthly statistics, it is also instructive to look at the effects of partial beamfilling on individual cloud cases. In this section, two cases are examined: a typical midtropospheric stratus cloud

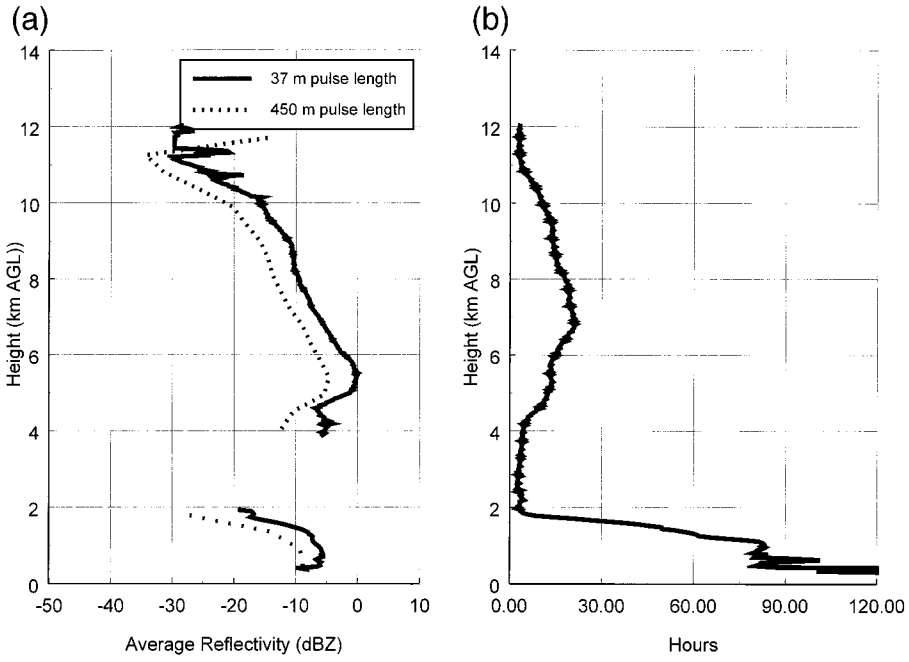

FIG. 9. As in Fig. 6 for ASTEX.

(FIRE II) and a shallow, marine boundary layer cloud (ASTEX).

1) MIDTROPOSPHERIC STRATUS CLOUD

A 30-min time–height cross section of a thick altostratus layer with possible embedded convection, complex multilayering, and a wide range of reflectivities (-40 to -10 dBZ) is presented in Fig. 11, and Fig. 12 shows the cumulative sums that have been calculated for reflectivities in 900-m range bins between 3.75 and 9.15 km. The solid line in Fig. 12 represents the statistics from the 37.5-m pulse length data, and the dotted lines represent the statistics from the virtual 450-m pulse length data. As would be expected for such a thick cloud, the most pronounced effect of range averaging

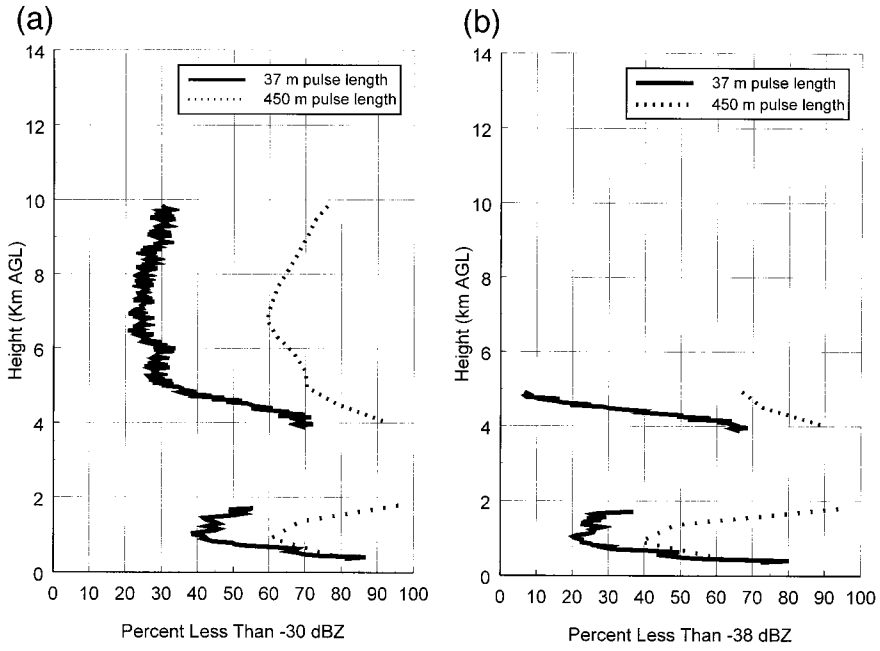

FIG. 10. As in Fig. 7 for ASTEX.

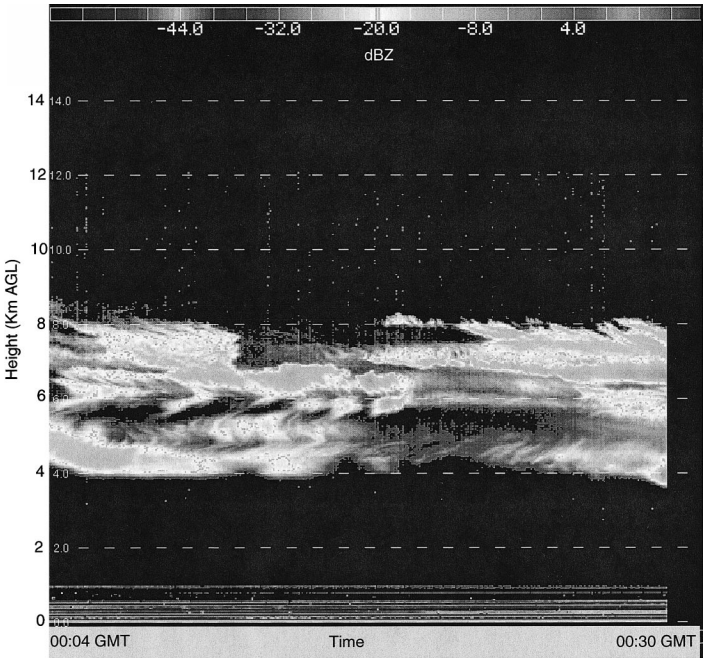

FIG. 11. Thirty-minute time–height cross section of radar reflectivities. Height axis ranges from 0 to 12 km, and time axis ranges from 0100 to 0130 UTC on 25 Nov 1991. Location is Coffeyville, Kansas.

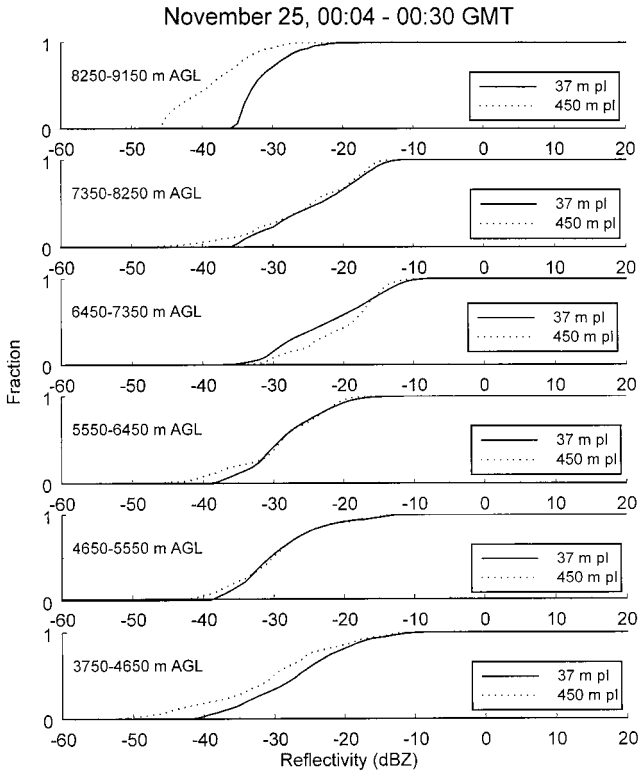

FIG. 12. Height-dependent cumulative sums of reflectivities for the cloud shown in Fig. 11 for 900-m range bins.

occurs at the cloud edges. At cloud base (between 3.75 and 4.65 km), the lowest measured reflectivity was around −41 dBZ; with the 450-m virtual pulse length, the lowest apparent reflectivity was −50 dBZ. For the range bins that are completely within the stratus deck (4.65 to 8.25 km), the beamfilling effects of a larger pulse length are minimal, despite the fact that the cloud is not solid and has some cloud-free gaps. At cloud top, where the 8.25 to 9.15 km range bin only had a very small amount of cloud, the effect is the most apparent, with the cumulative sums distributions from the 450-m pulse length data being significantly shifted to lower reflectivities compared to the 37.5-m pulse length data.

2) THIN BOUNDARY LAYER STRATUS CLOUD

An example of a shallow, low reflectivity (<−24 dBZ) marine stratus cloud of a type that was common and persistent during ASTEX is illustrated in Fig. 13. In this case, cumulative sums were calculated for 450-m range bins between 0.6 and 1.5 km and are shown in Fig. 14. As with Fig. 11, the solid lines show the cumulative sums of the reflectivities for the 37.5-m pulse length data, and the dotted lines show the cumulative sums of the reflectivities for the virtual 450-m pulse length data. In this case, the 0.6–1.05-km range bin is mostly filled with cloud, and the effect of the change in pulse length is small. For the 1.05–1.5-km bin, there is a substantial amount of cloud-free atmosphere (the highest cloud top is at 1.3 km, and average cloud-top height is nearer to 1.1 km), and this contrib-

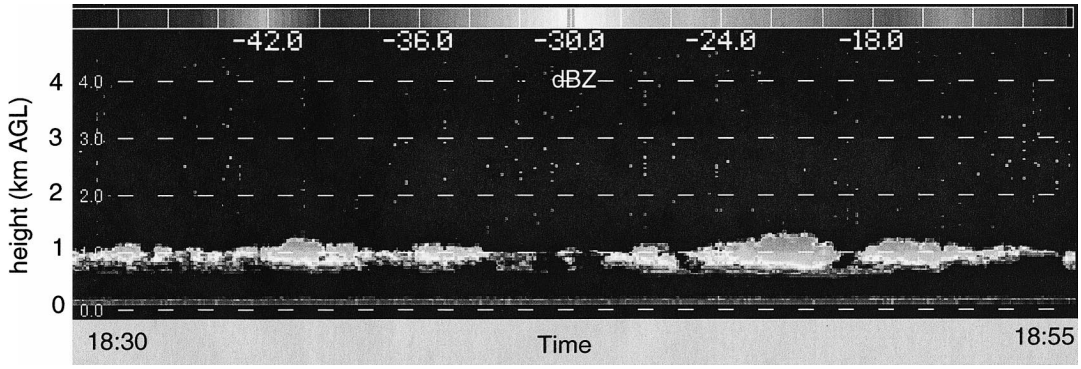

FIG. 13. Time–height cross section of radar reflectivity from 1830 to 1900 UTC on 13 Jun 1992 at Porto Santo Island, Portugal. Height axis ranges from 0 to 12 km.

utes to a cumulative sums distribution with much lower reflectivities for the 450-m pulse length data.

4. Discussion and summary

This study used two separate, month-long, ground-based radar datasets collected in significantly different cloud regimes to examine how increasing the radar pulse length can affect reflectivity statistics. These reflectivity statistics were examined with respect to a −30 dBZ threshold, which has been proposed as a feasible limit for a spaceborne radar, as well as with respect to a −38 dBZ threshold, which could be achieved for the same radar through pulse-coding techniques. The results are summarized in Table 2 for altitudes that were considered to be free of ground clutter and/or boundary layer targets (above 1 km for FIRE II and above 300 m for ASTEX). For clouds observed during the FIRE II experiment over wintertime Kansas, increasing the pulse length from 37.5 to 450 m decreased the fraction of detectable clouds by 21%–22% for both the −30 and the −38 dBZ minimum detectable thresholds. For ASTEX increasing the pulse length from 37.5 to 450 m decreased the fraction of detectable clouds by 38% for both the −30 and the −38 dBZ minimum detectable thresholds. The larger decreases in detectable clouds and the lower reflectivities in ASTEX result from the predominance of thin (relative to 450 m) marine stratus clouds in that dataset. Marine clouds are composed of small water droplets (low reflectivities) rather than large ice crystals (larger reflectivities), but because of their low altitude they are still detectable by the NOAA/K radar. Although some studies have indicated that clouds with reflectivities less than −30 dBZ are not radiatively significant, results here suggest that in some cases, geometrically thin clouds having actual reflectivities greater than −30 dBZ might be undetected by a low-resolution (450-m pulse length) radar because of the effects of partially filled pulse volumes.

In interpreting these results, several issues need to be considered. The table indicates that lowering minimum reflectivity thresholds to −38 dBZ could improve the fraction of detected clouds by 12%–15%. However, this gain would have to be achieved through pulse-coding techniques; in the lower 4 or 5 km of the atmosphere, the technique could not be applied because of incomplete information for pulse decoding caused by proximity to the ground resulting in significant range sidelobes. Therefore, pulse coding will be useful only in improving cloud detection in the upper atmosphere. Also, this study did not account for the attenuation effects that a space-based 94-GHz radar would encounter as opposed to the NOAA ETL 35-GHz system, which would cause some additional losses in the detection of thick, higher reflectivity clouds. Finally, the NOAA ETL system is not as sensitive as the unattended millimeter-wave cloud radars being presently operated by the Department of Energy (DOE) Atmospheric Radiation Measurement Program, and there was likely some fraction of clouds below its minimum detection levels that might have been detected by the DOE cloud radars or by lidars.

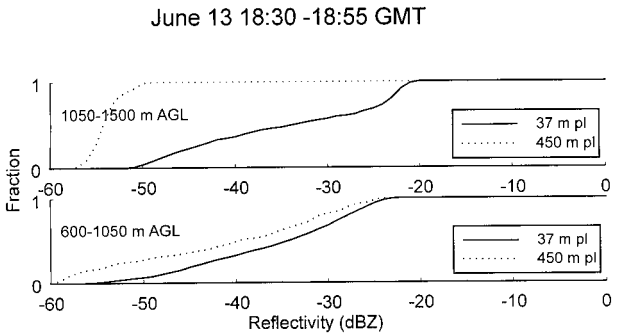

FIG. 14. Height-dependent cumulative sums of reflectivities for the cloud shown in Fig. 13 for 450-m range bins.

TABLE 2. Bulk reflectivity statistics for FIRE-II and ASTEX: 37.5-m and 450-m pulse lengths.

Pulse length	FIRE II <−30 dBZ	FIRE II <−38 dBZ	ASTEX <−30 dBZ	ASTEX <−38 dBZ
37.5-m	18%	4%	36%	24%
450-m	40%	25%	74%	62%

The net effect of these three factors indicate that the numbers presented in this study should be considered to be underestimates of the fraction of clouds that would be undersampled by a radar with a 500-m pulse length.

There are ameliorating factors that must also be considered. This study made no attempt to determine which of the clouds detected were radiatively significant, and it is these clouds that are the main focus of a space radar. Therefore, some fraction of clouds that this study determined to be undetectable by a long pulse length radar may be inconsequential, depending on the application. Also, the most recent plans are for a spaceborne lidar to fly in formation with a space radar (D.M. Winker 1999, personal communication). A space lidar will have much finer range resolution and in some conditions will be able to determine more precise cloud boundaries, which will be important in determining when partial beamfilling biases may be occurring for the radar, although the lidar will have a completely different set of problems associated with attenuation in thick and liquid clouds.

Also, with the recent advent of high sensitivity, continuously operating surface radars, the opportunity exists for the generation of extremely accurate, high-resolution reflectivity statistics from a few key sites. These surface-based sets will be invaluable for validating the spaceborne reflectivity statistics and creating a long-term database of potential biases. While spaceborne radars will provide the much needed global coverage of the vertical distribution of cloud reflectivities in the atmosphere, it will be the ground-based radars that will provide the information to extrapolate the ''tails'' of the distributions into the lower, but perhaps still important, reflectivity ranges.

This paper suggests several future studies. Similar statistics on radar reflectivities should be generated using the information from the 35-GHz cloud radars presently being operated by the DOE Atmospheric Radiation Measurement Program (Stokes and Schwartz 1994). These radars are presently operating in Alaska, Oklahoma, and on islands in the tropical western Pacific and similar radar has recently finished a year-long deployment as a part of the National Science Foundation Surface Heat and Budget of the Arctic program on the Arctic ice pack. Not only are these radars more sensitive than the NOAA/ETL 35-GHz radar used in this study, but they are operated in tandem with a sophisticated suite of radiation sensors, which can definitively determine which of the detected clouds are radiatively important. Another possibility for improved cloud detection from space would be to alter the operation plans for a spaceborne radar without making major design modifications. Rather than have the pulse volumes be contiguous, it is possible to overlap range sampling, that is, to sample the video signal at closer intervals than the transmitted pulse length. This would increase the probability that a thin cloud would be more completely sampled, and in addition, the weighted averages of the signal from the overlapping pulse volumes could be combined to construct more accurate statistics on the cloud reflectivities at cloud edges.

Space-based radar and lidar will be an undeniable asset in characterizing the vertical structure of clouds over the entire planet, which will be critical to understanding global radiation budgets. This study is based on a small enough sample of clouds that it is not possible to make a complete assessment of the present design specifications for a space-based radar in detecting clouds for radiation studies. However, because these results do suggest that pulse length issues may substantially affect cloud detection for some major cloud groups (boundary layer marine stratus and cirrus), it is essential that longer radar datasets from the ARM sites that are just becoming available be evaluated posthaste. This analysis will be essential in not only making decisions about last minute adjustments to the radar design specifications, but will also allow the operational biases to be compensated for once a space radar is in operation.

Acknowledgments. This study was supported by the NOAA Office of Global Programs, and the encouragement of Michael Coughlan in the early stages of this work was much appreciated. Radar data collection from the FIRE-II program was supported by NASA (NAG-1-1095). Radar data collection for the ASTEX program was supported by the NOAA Office of Global Programs, and partial support was received from NASA for radar shipping costs to Portugal. Tracey Sutherland and Kirk Walker provided valuable programing and data processing expertise during the analysis. This work would not have been possible without the engineering expertise of Bruce Bartram and Kurt Clark and the many long hours in the field put in by the NOAA/ETL radar group.

REFERENCES

Atlas, D., S. Y. Matrosov, A. J. Heysmfield, M. Chou, and D. B. Wolff, 1995: Radar and radiation properties of clouds. *J. Appl. Meteor.*, **34,** 2329–2345.

Brown, P. R. A., A. J. Illingworth, A. J. Heymsfield, G. M. McFarquhar, K. A. Browning, and M. Gosset, 1995: The role of spaceborne millimeter-wave radar in the global monitoring of ice clouds. *J. Appl. Meteor.*, **34,** 2346–2366.

Charlock, T., F. Rose, S.-K. Yang, T. Alberta, and G. Smith, 1992: An observational study of the interaction of clouds, radiation, and the general circulation. *Proceedings IRS'92: Current Problems in Atmospheric Radiation*, S. Keevallik and O. Karner, Eds., A. Deepak Publishing, 151–154.

——, ——, T. Albert, G. L. Smith, D. Rutan, N. Manola-Smith, P. Minnis, and B. Wielicki, 1994: Cloud profiling radar requirements: Perspective from retrievals of the surface and atmospheric radiation budget and studies of atmospheric energetics. *Utility and Feasibility of a Cloud of Profiling Radar, Report of the GEWEX Topical Workshop*, Pasadena, CA, IGPO Publication Series 10, WMO/TD-593, WCRP-84, 46 pp.

Clothiaux, E. E., M. A. Miller, B. A. Albrecht, T. P. Ackerman, J. Verlinde, D. M. Babb, R. M. Peters, and W. J. Syrett, 1995: An evaluation of a 94-GHz radar for remote sensing of cloud properties. *J. Atmos. Oceanic Technol.*, **12,** 201–228.

Fox, N. I., and A. J. Illingworth, 1997: The potential of spaceborne

cloud radar for the detection of stratocumulus clouds. *J. Appl. Meteor.*, **36,** 676–687.

IGPO, 1994: *Utility and Feasibility of a Cloud Profiling Radar, Report of the GEWEX Topical Workshop*, Pasadena, CA, IGPO Publication Series 10, WMO/TD-593, WCRP-84, 46 pp.

Kropfli, R. A., and R. D. Kelly, 1996: Meteorological research applications of MM-wave radar. *Meteorol. Atmos. Phys.*, **59,** 105–121.

——, and Coauthors, 1995: Cloud physics studies with 8 mm wavelength radar. *Atmos. Res.*, **35,** 299–313.

Lemke, H., O. Danne, M. Quanta, E. Raschke, R. A. Girard, and P. S. Park, 1997: Study on critical requirements for a cloud profiling radar. Executive Summary, ESTEC Contract No. 11327/94/NL/CN, GKSS Research Center, 10 pp.

Lhermitte, R. M., 1987: A 94-GHz Doppler radar for cloud observations. *J. Atmos. Oceanic Technol.*, **4,** 36–48.

Liang, X.-Z., and W.-C. Wang, 1997: Effect of cloud overlap on GCM climate simulations. *J. Geophys. Res.*, **102,** 11 039–11 047.

Mace, G. G., T. P. Ackerman, and E. E. Clothiaux, 1997: A study of composite cirrus morphology using data from a 94 Ghz radar and correlations with temperature and large-scale vertical motion. *J. Geophys. Res.*, **102** (D12), 13 581–13 593.

——, ——, P. Minnis, and D. F. Young, 1998: Cirrus layer microphysical properties derived from surface based millimeter radar and infrared interferometer data, 1998. *J. Geophys. Res.*, **103** (D18), 23 207–23 216.

Martner, B. E., and K. P. Moran, 2001: Using cloud radar polarization measurements to evaluate stratus cloud and insect echoes. *J. Geophys. Res.*, in press.

Moran, K. P., B. E. Martner, M. J. Post, R. A. Kropfli, D. C. Welsh, and K. B. Widener, 1998: An unattended cloud profiling radar for use in climate research. *Bull. Amer. Meteor. Soc.*, **79,** 443–455.

Schneider, T. L., and G. L. Stephens, 1996: Climatically relevant clouds as sensed by spaceborne cloud radar. *Proceedings of the International Radiation Symposium*, Deepak Publishing, 651–654.

Sekelsky, S. M., and R. E. McIntosh, 1996: Cloud observations with a polarimetric 33 Ghz and 95 Ghz radar. *Meteor. Atmos. Phys.*, **59,** 123–140.

Slingo, A., and J. M. Slingo, 1988: The response of a general circulation model to cloud longwave radiative forcing. I: Introduction and initial experiments. *Quart. J. Roy. Meteor. Soc.*, **114,** 1027–1062.

Stackhouse, P. W., Jr., and G. L. Stephens, 1991: A theoretical and observational study of the radiative properties of cirrus: Results from FIRE 1986. *J. Atmos. Sci.*, **48,** 2044–2059.

Stephens, G. L., and P. J. Webster, 1984: Cloud decoupling of the surface and planetary radiative budgets. *J. Atmos. Sci.*, **41,** 681–686.

Stokes, G. M., and S. E. Schwartz, 1994: The Atmospheric Radiation Measurement (ARM) Program: Programmatic background and design of the cloud and radiation test bed. *Bull. Amer. Meteor. Soc.*, **75,** 1201–1221.

Uttal, T., E. E. Clothiaux, T. P. Ackerman, J. M. Intrieri, and W. L. Eberhard, 1995: Cloud boundary statistics during FIRE II. *J. Atmos. Sci.*, **52,** 4276–4284.

Walter, S. J., G. L. Stephens, and D. G. Vane, 1998: The CLOUDSAT mission. *Proc. Battle Space Atmosphere and Coud Impacts on Military Operations Conf*., Hanscom AFB, MA, Air Force Research Laboratory, 139–145.